the broadside direction. Although the cross-polarisation is quite high in the direction around $\theta = 30°$, its value is below –20dB in the boresight.

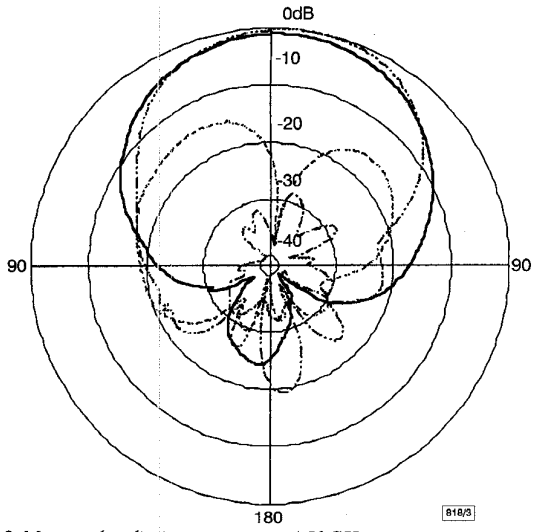

Fig. 3 *Measured radiation patterns at 4.53GHz*

——— H-co-polarisation
– – – – H-cross-polarisation
— ·· — E-co-polarisation
— · — · E-cross-polarisation

Discussion: The performance of this L-probe microstrip antenna is quite similar to the U-slot microstrip antenna, in the sense that both exhibit wideband and high gain characteristics. (The bandwidth of the L-probe patch (~28%) is slightly less than that of the U-slot patch (~32%) when both have the same thickness, H = 5mm).

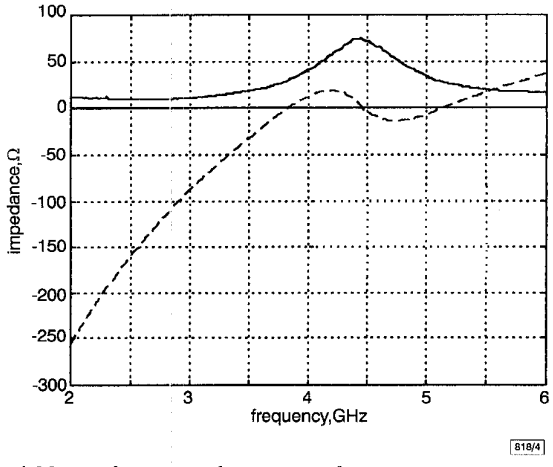

Fig. 4 *Measured input impedance against frequency*

——— real
– – – – imaginary

The vertical portion of the L-shaped probe forms an open circuit stub of length less than a quarter of the wavelength with the patch (capacitive). Together with the inductance of the horizontal portion of the L-probe, the stub acts as a series-resonant element with a resonant frequency close to that of the TM_{01} mode of the patch. The conventional probe acts only as an inductor which deteriorates the bandwidth performance of the microstrip antenna. This is clearly shown in Fig. 4. Also, similar to the U-slot patch antenna, the cross-polarisation caused by the horizontal arm of the probe may be quite high in certain applications, even though it is slightly less than that of the U-slot patch. Preliminary results indicated that the cross-polarisation can be reduced in some array environments [7]. Detailed results will be presented elsewhere.

3 June 1998
Electronics Letters Online No: 19981009

K.M. Luk, C.L. Mak and Y.L. Chow (*Department of Electronic Engineering, City University of Hong Kong, 83 Tat Chee Avenue, Kowloon, Hong Kong*)

K.F. Lee (*Department of Electrical Engineering, University of Missouri-Columbia, Engineering Building West, Columbia, Missouri 65211, USA*)

References

1 LEE, R.Q., LEE, K.F., and BOBINCHAK, J.: 'Characteristics of two-layer electromagnetically coupled rectangular patch antenna', *Electron. Lett.*, 1987, **23**, pp. 1070–1072
2 CHANG, E., LONG, S.A., and RICHARDS, W.F.: 'Experimental investigation of electrically thick rectangular microstrip antennas', *IEEE Trans.*, 1986, **AP-34**, pp. 767–772
3 AU, T.M., TONG, K.F., and LUK, K.M.: 'Characteristics of aperture-coupled co-planar microstrip subarrays', *IEE Proc. Microw. Antennas Propag.*, 1997, **144**, pp. 137–140
4 HALL, P.S.: 'Probe compensation in thick microstrip patches', *Electron. Lett.*, 1987, **23**, pp. 606–607
5 LEE, K.F., LUK, K.M., TONG, K.F., SHUM, S.M., HUYNH, T., and LEE, R.Q.: 'Experimental and simulation studies of coaxially fed U-slot rectangular patch antenna', *IEE Proc. Microw. Antennas Propag.*, 1997, **144**, pp. 354–358
6 NAKANO, H., YAMAZAKI, M., and YAMAUCHI, J.: 'Electromagnetically coupled curl antenna', *Electron. Lett.*, 1997, **33**, pp. 1003–1004
7 HUANG, J.: 'A parallel-series-fed microstrip array with high efficiency and low cross-polarization', *Microw. Opt. Technol. Lett.*, 1992, **5**, pp. 230–233

Iterative network model to predict the behaviour of a Sierpinski fractal network

C. Borja, C. Puente and A. Medina

A simple, fast, numerical model to predict the input parameters of a network with the topology of the Sierpinski gasket fractal shape, is introduced. The usefulness of the model is shown through comparison with experimental results for the SPK90 patch antenna.

Introduction: The use of fractal structures in the design of antennas has been described recently [1 – 4]. Antennas based on the Sierpinski gasket fractal shape (also the Sierpinski triangle) present logperiodic behaviour on both the input parameters and radiation patterns. The aim of this work is two-fold: first, a simple numerical method is introduced to predict the overall frequency behaviour of a fractal antenna or network, and secondly, the method is based on a recursive model which demonstrates that the multiband properties of such a fractal network are tightly linked to the fractal nature of its structure. Also, since the electromagnetic analysis of fractal shapes usually consumers large amounts of memory and computing time, the simple model is also very useful in the design process when extremely fast estimation of the global tendencies is required. The application of such a model to the prediction of the behaviour of a fractal patch antenna is also illustrated.

Iterative network model : The iterative network model is a simple, fast, numerical model that predicts the input parameters (input reflection coefficient and input impedance) of an antenna or circuit whose topology is that of the Sierpinski gasket fractal shape. The model is based on the same recursive principle used to generate fractal structures (iterated function systems, IFSs). An IFS system is a feedback system where the system output is considered as the new system input at the next stage.

This model uses only two basic relations in order to predict the input parameters of the fractal network: the scattering matrix of the initial structure (the *initiator* in fractal terminology), and the generator constitutive relations that link the [S] matrix of a particular stage of the fractal construction to the [S′] matrix of the next stage.

The procedure for computing the whole scattering matrix is as shown in Fig. 1. This procedure applies a T[ ] transformation, which characterises the basic algorithm stage, as many times as

fractal iterations are used to form the total structure. In this procedure, the output is considered as a new input, except at the beginning of the algorithm where the input is the scattering matrix of the initiator.

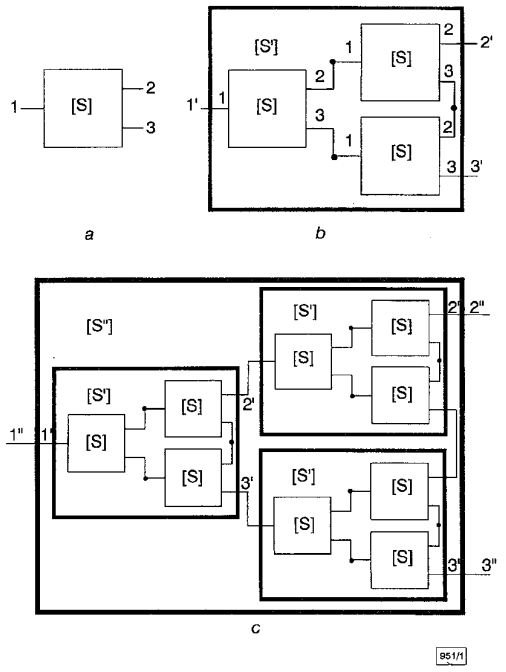

Fig. 1 *Scheme of iterative network model*

a Basic structure
b Basic stage
c Topology of Sierpinski fractal

For an equilateral gasket, the [S] matrix of the initial structure is fully characterised by the parameters α and β (eqn. 1) owing to the reciprocity and symmetry properties:

$$[S] = \begin{bmatrix} \alpha & \beta & \beta \\ \beta & \alpha & \beta \\ \beta & \beta & \alpha \end{bmatrix} \quad (1)$$

The geometry of the basic stage (Fig. 1*b*) and the form of the scattering matrix (eqn. 1) allow us to deduce the [S'] matrix associated with the basic stage, which is also a three-port network with an [S] matrix equal to eqn. 1 but with parameters $\alpha'$and β'. Such parameters (α_{n+1} and β_{n+1}) are related to those of the previous stage (α_n and β_n) through the equations:

$$\alpha_{n+1} = \alpha_n + \frac{2\beta_n^2\left(\alpha_n + \frac{\beta_n^2}{1-\alpha_n}\right)}{1-(\alpha_n+\beta_n)\left(\alpha_n + \frac{\beta_n^2}{1-\alpha_n}\right)} \quad (2)$$

$$\beta'_{n+1} = \frac{\beta_n^2\left(\alpha_n + \frac{\beta_n}{1-\alpha_n}\right)}{1-(\alpha_n+\beta_n)\left(\alpha_n + \frac{\beta_n^2}{1-\alpha_n}\right)} \quad (3)$$

Analogous relations (with a rather involved appearance) for non-equilateral triangle initiators have also been derived [4]. It is interesting to stress that the recursive relations of eqns. 2 and 3 allow us to predict the network behaviour at any iteration stage without an increase in the model complexity, since only two parameters are stored regardless of the number of iterations.

Experimental and computed results: The usefulness and accuracy of the model are shown through comparison with experimental results (Fig. 3) for the SPK90 patch antenna (Fig. 2). A symmetrical Y junction of lossy transmission lines was used to model the fractal initiator (Fig. 2). The reflection coefficient of the SPK90 patch is calculated when the value of the three transmission lines quality factor (Q) is 100 in one case (Fig. 3*a*) and 10 in the other (Fig. 3*c*). The patch antenna was printed over a Cuclad 250 dielectric substrate (ε_r = 2.5, h = 1.588mm). Its input reflection coefficient (Γ_{in}) relative to 50Ω was measured from 200 to 18MHz using an HP8510B. The patch input reflection coefficient is measured for two values of the h parameter (separation between the ground plane and the patch surface), that is h = 1.588mm (Fig. 3*b*) and h = 14.4mm (Fig. 3*d*). For the case where Q = 10, Fig. 3*c* clearly shows logperiodic behaviour with the logperiod (δ) being approximately a factor of two. In contrast, Fig. 3*a* (Q = 100) does not show logperiodic behaviour as clearly as Fig. 3*c*. This phenomenon also appears in the measured reflection coefficient (Fig. 3*b* and *d*), i.e. when the value of the h separation increases so that Q of the patch is lowered, the logperiodic behaviour is clearer. Thus, it can be concluded that attenuation (for instance by the radiation process) is important to enhance log-periodic behaviour. The deviation of the experimental results at high frequencies for the low Q case is due to the non-negligible contribution of the coaxial probe for a large separation between the patch and the ground plane.

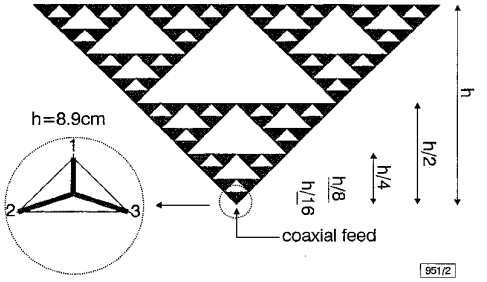

Fig. 2 *SPK90 patch, and Y model for transmission lines that compose initial structure*

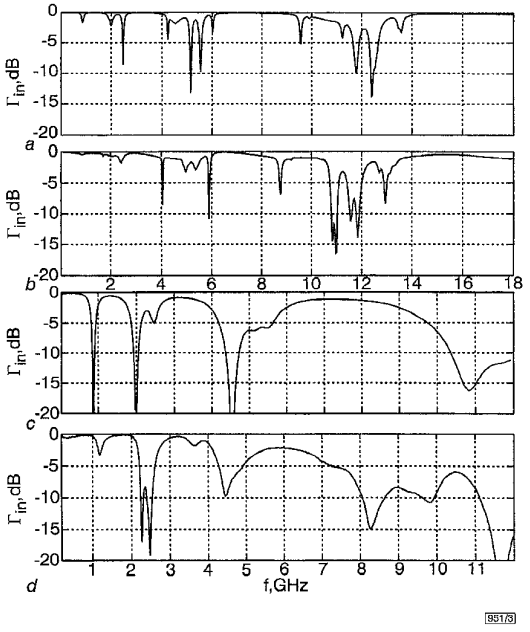

Fig. 3 *Input reflection coefficient of SPK90 patch*

a Simulated with iterative network model for transmission lines with Q = 100
b Measured for h = 1.58 mm
c Simulated with iterative network model for Q = 10
d Measured for h = 14.4 mm

Conclusions: The iterative network model yields extremely fast prediction of the behaviour of a network or antenna whose topology is that of the Sierpinski gasket fractal shape. The model is especially useful when the number of iterations is high and an overall behaviour is investigated. The model appears useful for determining conclusions for the design of fractal patch antennas as well, namely that a low Q enhances the logperiodic behaviour of the antenna.

Acknowledgments: This work has been partially supported by the Spanish government through grant number TIC-96-0724-C06-04, and by the companies Sistemas radiantes F. Moyano and Fractus. Fractal antennas are patent pending.

9 June 1998
Electronics Letters Online No: 19981020

C. Borja, C. Puente and A. Medina (*Electromagnetics and Photonics Engineering Group, Department of Signal Theory and Communications, Universitat Politècnica de Catalunya (UPC), c/Gran Capità s/n, Modul D3 Campus Nord UPC, 08034 Barcelona, Spain*)

E-mail: puente@tsc.upc.es

References

1 PUENTE, C., ROMEU, J., POUS, R., GARCIA, X., and BENITEZ, F.: 'Fractal multiband antenna based on the Sierpinski gasket', *Electron. Lett.*, 1996, **32**, (1), pp. 1–2

2 PUENTE, C., ROMEU, J., POUS, R., and CARDAMA, A.: 'On the behaviour of the Sierpinski multiband fractal antenna', *IEEE Trans. Antennas and Propagation*, September 1996, (submitted)

3 PUENTE, C., ROMEU, J., BARTOLOMÉ, J., and POUS, R.: 'Perturbation of the Sierpinski antenna to allocate operating bands', *Electron. Lett.*, 1996, **32**, (24), pp. 2186–2188

4 PUENTE, C.: 'Fractal antennas'. Doctoral Thesis at the Dept. of Signal Theory and Communications, Universitat Politècnica de Catalunya, June 1997

Charge pump boosting technique for power noise immune high-speed PLL implementation

Kwangho Yoon and Wonchan Kim

A phase-locked (PLL) with a charge pump boosting technique is described. The technique enables the voltage controlled oscillator circuit in the PLL to run faster than conventional circuits at low supply voltage. This design method is applicable to PLLs with low jitter, high-speed characteristics in environments with high supply noise.

Introduction: In a mixed-mode signal environment, the most important problem is the production of supply noise caused by the switching of digital gates. This makes the design of a high-speed phase-locked (PLL) with low jitter characteristics very difficult. The most widely used design method for reducing the PLL jitter in such a noisy environment has been to employ a differential voltage controlled oscillator (VCO) with good noise rejection. However, this cannot alleviate the problem of coupling the power supply noise directly to the VCO output node through parasitic capacitances. An attractive approach was proposed recently which attempted to isolate the VCO from the noisy supply. This approach employed a source follower and its effectiveness was demonstrated [1]. However, it suffers from a large voltage drop which results from the source follower severely reducing the maximum operating frequency of the VCO in the PLL. To solve this problem of voltage drop, we propose a charge pump boosting technique. The basic idea of this technique is to reduce the unnecessarily large noise margin of the source follower. Then, the oscillation frequency of the VCO can be increased again. This charge pump boosting technique is applied to a high-speed, low jitter PLL that can be operated with power supply noises of large magnitude. For an effective implementation of such a PLL we also developed a new precharge type dynamic phase frequency detector (PFD).

Charge pump boosting technique: Fig. 1 shows a block diagram of the PLL with charge pump boosting technique. The principle feature of this circuit is that the oscillation frequency of the VCO is controlled by the supply voltage to the VCO. Without the boosting circuit, the maximum loop filter voltage V_{ctrl} would be near V_{dd} and the actual supply voltage transferred to the VCO would be only $V_{dd} - V_{gs}$. This V_{gs} voltage drop severely decreases the maximum operating frequency of the VCO, resulting in an excessive noise margin. By inserting a charge pump boosting circuit, we can increase the loop filter voltage V_{ctrl} above V_{dd} as long as the source follower M_1 operates in the saturation region for supply noise rejection. Hence, the maximum V_{ctrl} becomes $V_{dd} + V_t$ when no power supply noise exists. Considering power supply noise of amplitude V_n, the maximum V_{ctrl} becomes $V_{dd} + V_t - V_n$, to leave room for noise rejection of amplitude V_n. Owing to the switching operation of the charge pump circuit, the noise of the boosting circuit is not transferred to the loop filter. Therefore, there is no degradation of the jitter characteristics of the PLL, which is verified by experimental results to be discussed later.

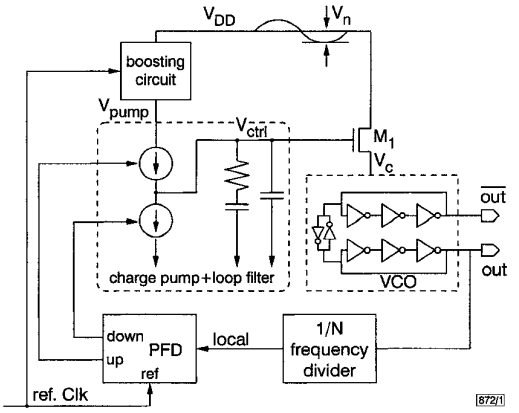

Fig. 1 *Charge pump boosting PLL block diagram including schematic diagram of VCO*

Design of PLL blocks: For our charge pump boosting PLL, the most suitable form of VCO is the classical ring oscillator with CMOS inverters as delay elements. This is because the oscillation frequency is almost linearly controlled by the supply voltage [2]. The differential VCO is not suitable, as the oscillation frequency is nearly independent of supply voltage in its operating principle. A supply voltage-controlled VCO which can output differential phase is shown in Fig. 1. It is composed of two single-ended three stage ring oscillators. The inverter cross-coupling method used here achieves a 180° phase shift between each independent ring oscillator without decreasing the maximum operating frequency. The PFD in the PLL detects the phase and frequency differences between the reference frequency and the local oscillator frequency.

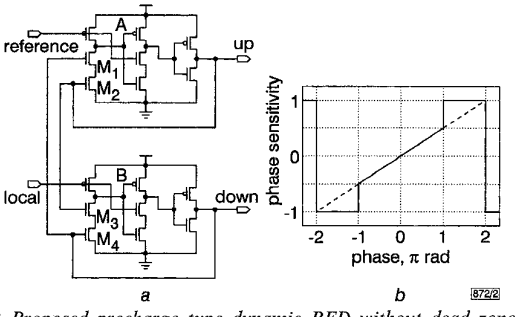

Fig. 2 *Proposed precharge type dynamic PFD without dead zone and phase characteristic of conventional and proposed PFDs*

a Proposed precharge type dynamic PFD without dead zone
b Phase characteristics
– – – – conventional PFD
——— proposed PFD

A PFD is usually built with a state machine with memory elements such as flip-flops. However, such a static PFD requires many logic gates which limits high-speed operation. More advanced versions use dynamic logic for high-speed operation and small area [3], but this type of precharge PFD suffers from the drawback of a dead zone in the phase characteristic at the equilibrium point. We propose a dead zone-free, dynamic PFD composed of a minimum number of transistors, as shown in Fig. 2*a*. This PFD generates an up and down pulse signal of sufficient width when two input phases are locked. Hence, the dead zone is eliminated without the insertion of a delay element in the feedback path of the PFD. The most distinguishing difference in phase characteristic between the conventional PFD and proposed precharge type of PFD is that the phase sensitivity jump occurs at π and $-\pi$ as, shown in Fig. 2*b*. This phase characteristic of the proposed PFD slightly decreases the locking time of the PLL compared to that using the conventional PFD.